

## **NOTICE CONCERNING COPYRIGHT RESTRICTIONS**

This document may contain copyrighted materials. These materials have been made available for use in research, teaching, and private study, but may not be used for any commercial purpose. Users may not otherwise copy, reproduce, retransmit, distribute, publish, commercially exploit or otherwise transfer any material.

The copyright law of the United States (Title 17, United States Code) governs the making of photocopies or other reproductions of copyrighted material.

Under certain conditions specified in the law, libraries and archives are authorized to furnish a photocopy or other reproduction. One of these specific conditions is that the photocopy or reproduction is not to be "used for any purpose other than private study, scholarship, or research." If a user makes a request for, or later uses, a photocopy or reproduction for purposes in excess of "fair use," that user may be liable for copyright infringement.

This institution reserves the right to refuse to accept a copying order if, in its judgment, fulfillment of the order would involve violation of copyright law.

## FRACTAL ANALYSIS AND MODELING OF A TWO-DIMENSIONAL FRACTURE NETWORK IN A GEOTHERMAL RESERVOIR

Noriyoshi Tsuchiya and Katsuto Nakatsuka

Department of Resources Engineering, Faculty of Engineering,  
Tohoku University, Sendai 980-77, Japan

### ABSTRACT

The space filling fractal dimension and geometric features of outcropping fractures in the Tamagawa Welded Tuffs in the Kakkonda geothermal area, Northeast Japan, and artificial 2D network models have been investigated. The fracture space filling fractal dimension was determined using the box-counting method, and several geometric characteristics including length distribution, orientation, connectivity, number of fractures, and total length of fractures were quantified in order to construct a two-dimensional fracture network model. The fractal dimension of fracture space filling observed in 0.5m square areas was found to be proportional to the number of fractures in the maximum cluster. The number of junctions, fractures, and total length of all fractures were also connected to the fractal dimension. Computer-generated two-dimensional fracture network patterns utilising the observed fractal dimension and geometric relationships can simulate natural fracture patterns.



Fig.1 Index map of study area.

### INTRODUCTION

Fractured reservoir concepts have received considerable attention in order to model the formation and circulation of geothermal reservoirs. The fracture network in reservoir host rocks has been assumed to be well connected and equivalent to a homogeneous medium. However, Fractal geometry is the description of forms more complex than the standard Euclidean shapes. A fractal form is characterized by its fractal dimension, which is greater than its topological dimension.

Considerable work has been done to describe the fractal characteristics of shape and surface topologies of fractures (Katz and Thompson, 1983; Tsang and Witherspoon, 1983; Brown and Scholtz, 1985(a),(b); Vaughan et al., 1986). Space filling and length distribution of fractures have also been identified as fractal (Main et al., 1990; Ledésert et al., 1993; Tsuchiya et al., 1994). Further, Chang and Yortsos (1990) have calculated the pressure-transient response of single-phase flow in a fractal object. Watanabe and Takahashi (1995) evaluated heat extraction capacity using a purely random model consisting of line segments and/or round disks.

Fractal geometry is therefore a natural candidate for the representation and modeling of multi-fracture systems in geothermal reservoirs. Natural-like reservoir models are required in order to characterize better the heat and fluid transfer in geothermal reservoirs.

The purpose of this study is to characterize natural fracture networks in 2D using the space filling fractal dimension together with certain geometric features and then to model the fracture network using these parameters.

### SAMPLE AND NATURAL FRACTURE PATTERN

The Tamagawa Welded Tuffs are mainly composed of rhyolitic and dacitic welded tuffs dated between 0.7 to 3.6Ma using fission track and K-Ar dating methods (Tamanyu and Lanphere, 1983). The Tamagawa Welded Tuffs are one of the main cap rocks and/or reservoir rocks in the Kakkonda (Takinoue) and Matsukawa geothermal areas in northern Honshu, Japan (Fig.1).

Fractures observed in 0.5m x 0.5m outcrops were traced onto a transparent vinyl sheet. The ratio between tracing resolution which is about 1cm ( $l_{min}$ ), and the length of the side of the square sheet  $R_{0.5}$  is 0.02 ( $l_{min}/R_{0.5}$ ). Fifteen sheets were traced from Tamagawa Welded Tuffs outcrops for fractal analysis and for the geometric characterization of fracture patterns.

### FRACTAL DIMENSION OF SPACE FILLING

Fig.2(a) shows an example of the fracture pattern from a 0.5m square observation area. Fractal dimension of fracture space filling,  $D_f$ , was obtained by means of the box-counting algorithm (Klinkenberg, 1994). Using this method ratios of the cell size  $r$  to  $R_{0.5}$  are 0.02, 0.04, 0.1, and 0.2. In other words, lower and upper cutoff levels for calculating fractal dimension are 0.02 and 0.2 respectively. The lower cutoff level  $r_{min}/R_{0.5}$  is equal to the  $l_{min}/R_{0.5}$  as mentioned above. Fig.2(b) shows a log-log plot of the number of cells covered with fracture against cell dimension. Linearity of the number of cells against cell size is well recognized within the 0.2 to 0.02 range, and the slope of the straight line indicates the space filling fractal dimension which is 1.32. The space filling fractal dimension of all natural fracture patterns used in this study ranges from 1.08 to 1.48 with a mean value of 1.23.

Tsuchiya et al. (1994) presented fractal dimensions of fracture space filling  $D_f$  at different length scales. The mean values of  $D_f$  were 1.28 for both 1.6mm and 10m square observation areas. These results suggested that the fractal dimension of fracture space filling of zoom sequences from microscopic to 10 meter order have a single fractal property.

### GEOMETRICAL CHARACTERISTICS

The selected geometrical features listed in Table1 were obtained from the natural fracture patterns. The length of fracture and/or fracture segment were defined as the number of the minimum cells, 1cm square, covering the fracture. Orientation distribution was measured in the direction of the line between the start and end points of fracture segment. The natural fractures were classified into connected clusters. (Odling, 1992). Fig.3 shows schematic

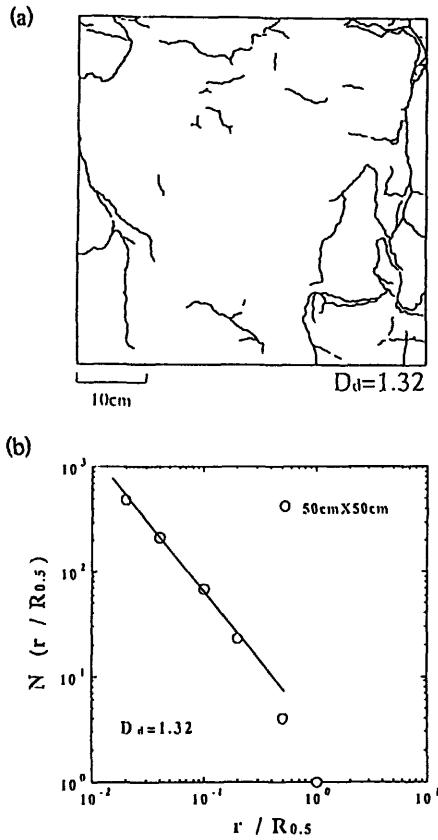


Fig.2 (a) An example of the natural fracture pattern in 0.5m square area, (b) the relationship between  $r / R_{0.5}$  and the number of cells crossed by fractures.

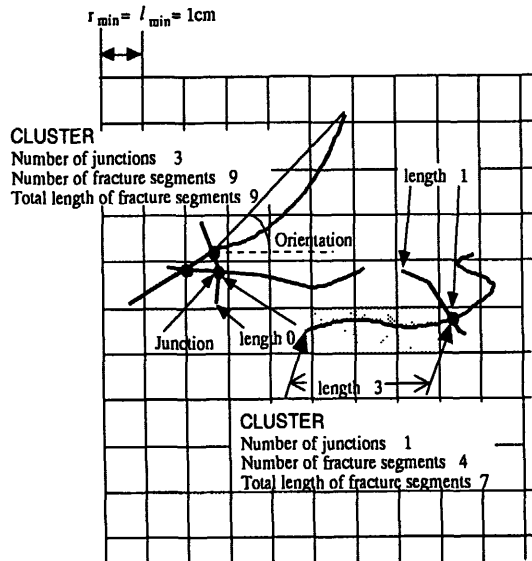


Fig.3 Explanation of definition of cluster, orientation and fracture length.

Table 1 Selected parameters for modeling.

Fractal dimension of fracture space filling
Fractal dimension of fracture shape
Length distribution
Orientation
Number of fractures in the maximum cluster in the other clusters
Number of junctions
Total length of all fractures
Segment length between junctions.
Number of cells covering single fracture

illustration of the definition of cluster, orientation and fracture length. On the basis of the definition of fracture length, if a fracture crosses over minimum one cell, the length is counted as unity, and if a fracture doesn't cross throughout the cell, that cell is omitted for counting length. For example, even if one fracture is distributed over five cells, the length is defined as 3 shown by shaded cells in Fig.3.

Fig.4 shows a histogram of length distribution. The x-axis is the number of cells covering a single fracture and/or fracture segment. Fractures of length 2 are commonest, and the frequency decreases exponentially with increasing length.

The size of the maximum cluster, that containing the largest number of fractures, strongly affects the fractal dimension of fracture space filling and the visual impression of the fracture pattern. Relationships between the fractal dimension and the geometric parameters were examined to facilitate generation of the fracture network models.

Fig.5 shows relationship between fractal dimension  $D_d$  and number of fractures in the maximum cluster (cluster<sub>max</sub>). Data is approximated by the

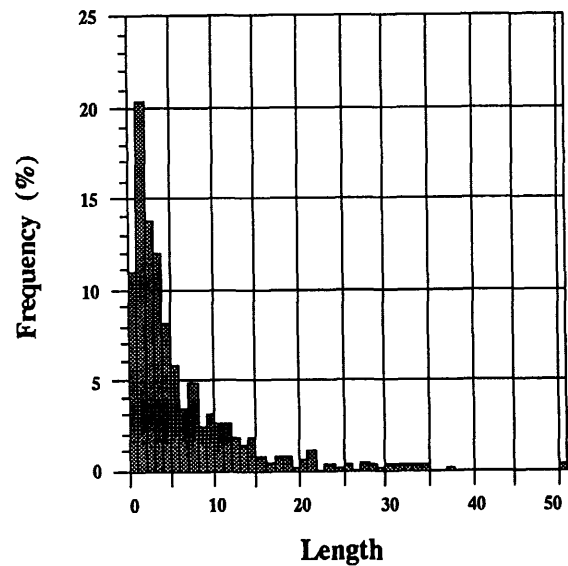


Fig.4 Length distribution.

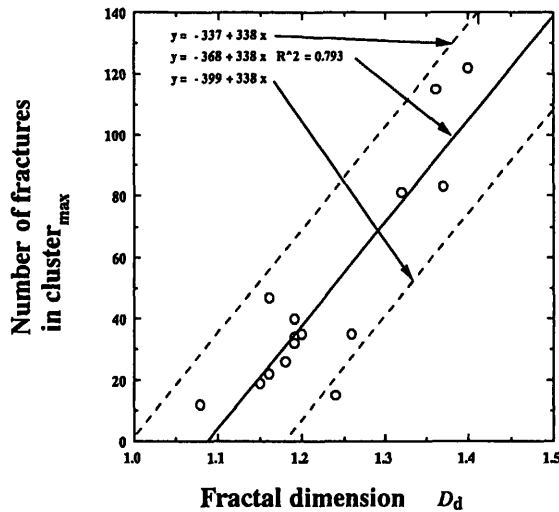


Fig.5 Relationship between fractal dimension and number of fractures in the maximum cluster.

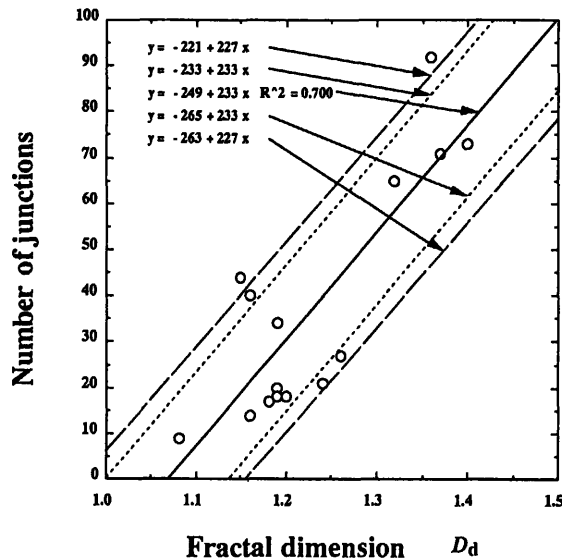


Fig.6 Relationship between fractal dimension and number of junctions.

solid straight line, and the broken lines are defined by following hypotheses:  
 a) The number of fractures is unity, when dimension is unity. b) Broken lines have the same slope as the approximation line and are symmetric with respect to the approximation line.

Fig.6 shows the relationship between fractal dimension and the number of junctions. The data is approximated by a solid line. The upper dotted line has the same slope as that of the approximation line and passes through the point (1.0, 0.0). This means that number of junctions is zero when fractal dimension is unity. The lower dotted line is symmetric about the approximation line.

Fig.7 plots number of junctions against number of fractures in the maximum cluster. The two geometric parameters have an adequate correlation, therefore, the number of junctions, the number of fractures in cluster<sub>max</sub> and the fractal dimension are correlated to each other.

The number of fractures in cluster<sub>max</sub> was selected in the range between the broken lines in Fig.5 for a given fractal dimension. This value can be

converted into the number of junctions using the correlation shown in Fig.7. The broken lines in Fig.6 indicate upper and lower limits of the number of junctions calculated on the basis of the number of fractures in cluster<sub>max</sub>. The broken line range encloses the area covered with the dotted lines in Fig.6. Therefore, the number of junctions determined in Figs.5 & 7 for a given fractal dimension always satisfies the relation between number of junctions and fractal dimension in Fig.6.

Fig.8 shows the relationship between fractal dimension and the number of fractures in the whole patterns. The number of fractures as a function of the number of fractures in cluster<sub>max</sub> is shown in Fig.9, and relation between the number of junctions and the number of fractures is presented in Fig.10. Using these mutual correlations we can get a possible range for the number of fractures following the steps given below.

- step 1 Determination of the upper and lower limits of number of fractures in the maximum cluster for a given fractal dimension using the broken lines in Fig.5.
- step 2 Conversion of the upper and lower limits of the number in cluster<sub>max</sub> into the number of junctions using Fig.7.
- step 3 Conversion of the fracture numbers in cluster<sub>max</sub> into the number of fractures using Fig.9.
- step 4 Conversion of the number of junctions calculated in step2 into the number of fractures using Fig.10.
- step 5 Determination of the upper and lower limits of the number of fractures for a given fractal dimension.

The broken lines in Fig.8 represents calculated results of steps 1 & 3. The dotted line is from steps 2 & 4, and the bold lines indicate a possible range of the number of fractures for a given fractal dimension satisfying the mutual correlations.

Fig.11 shows the relationship between the fractal dimension and the total length of all fractures in whole fracture patterns. The total length is presented as functions of the number of fractures in cluster<sub>max</sub>, number of junctions and number of fractures in Figs.12-14. The possible range of the total length is estimated by following steps similar to the above procedure:

- step 6 Conversion of the number of fractures in cluster<sub>max</sub> obtained from step 1 into the total length of all fractures using Fig.12.
- step 7 Conversion of the number of junctions of step 2 into the total length using Fig.13.
- step 8 Conversion of the number of fractures calculated in step5 into the total length using Fig.14.

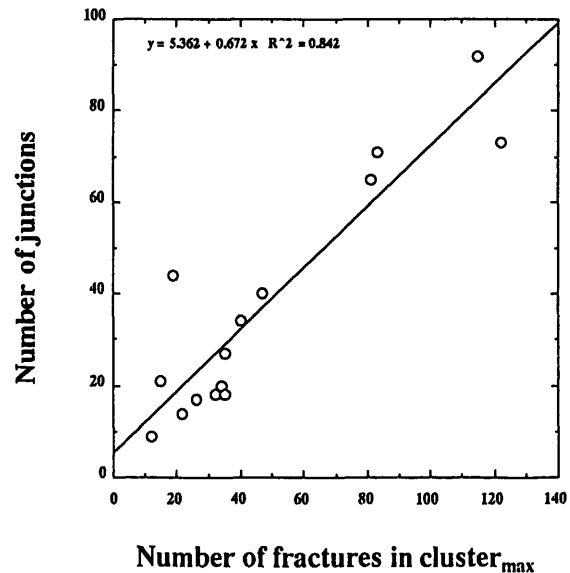


Fig.7 Relationship between number of fractures in the maximum cluster and

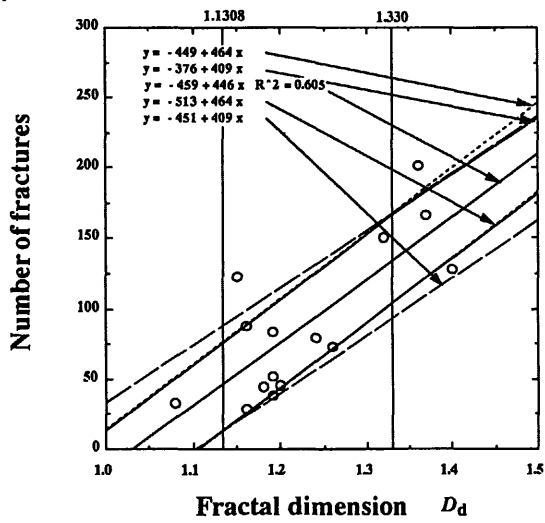


Fig.8 Relationship between fractal dimension and number of fractures.

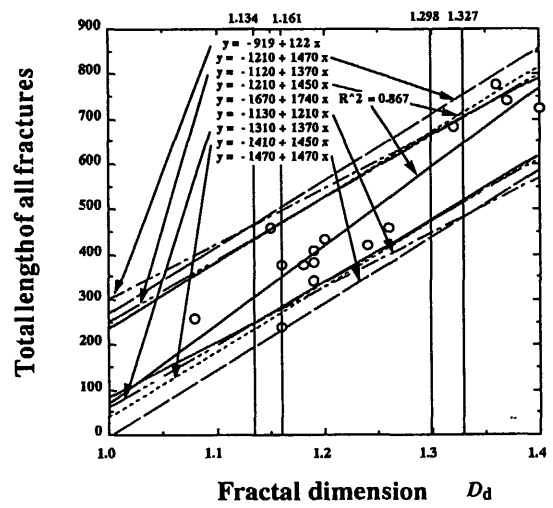


Fig.11 Relationship between fractal dimension and total length of all fractures.

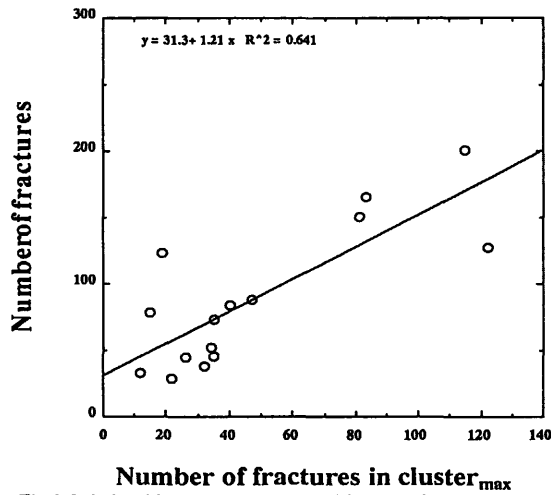


Fig.9 Relationship between number of fractures in the maximum cluster and number of fractures.

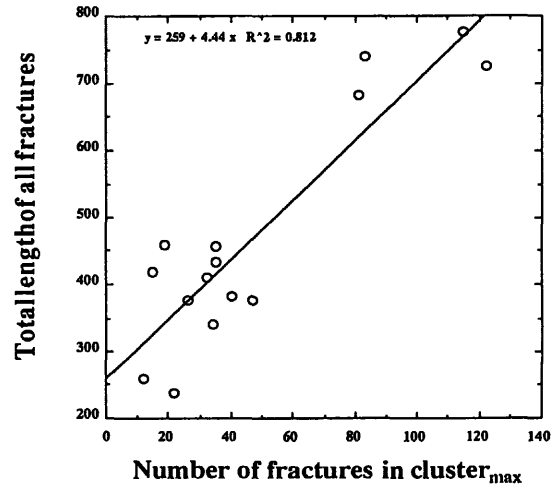


Fig.12 Relationship between number of fractures in the maximum cluster and total length of all fractures.

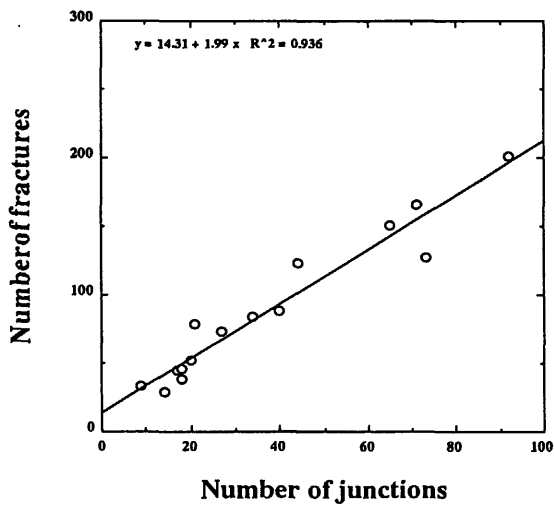


Fig.10 Relationship between number of junctions and number of fractures.

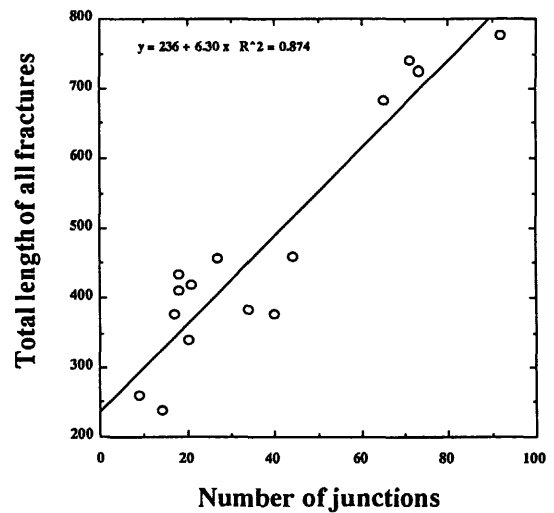


Fig.13 Relationship between number of junctions and total number of all fractures.

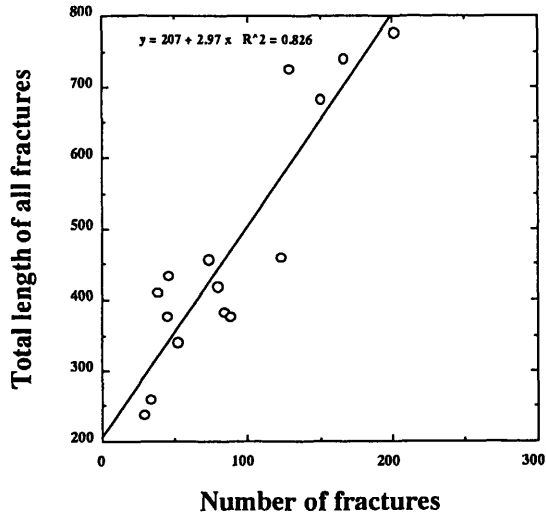


Fig.14 Relationship between number of fractures and total length of all fractures.

- step 9 Conversion of the number of fractures of step 3 into the total length using Fig.14.
- step 10 Determination of upper and lower limits of the total length of all fractures for a given fractal dimension.

The broken lines in Fig.11 shows the results of step 6, dotted line step7, chained line step8, and two-dot-dash line is from step 9. The minimum area satisfying all restrictions is enclosed by the bold lines and shown in Fig.11.

TWO-DIMENSIONAL FRACTURE NETWORK MODEL

Fig.15 is a flow chart for the computer generation of a fracture network model. The number of fractures in cluster<sub>max</sub> was selected randomly within the broken lines in Fig.5 for an input fractal dimension. After that, the number of junctions was determined randomly within the dotted lines in Fig.6 for an input fractal dimension. This value for junctions always satisfies the relationship between fractal dimension and the number of fractures in cluster<sub>max</sub>. The number of fractures in whole network pattern was obtained randomly within the broken lines in Fig.8 for an input fractal dimension. The parameters such as the number of fractures in the maximum cluster, the number of junctions and the number of fractures can be selected independently.

These selected data are merely information about the number of fractures. As the next step, it is necessary to assign length to each fracture on the basis of length distribution shown in Fig.4. However, the total length is also connected and restricted by the other geometric parameters. If the calculated total length lies outside the broken lines range shown in Fig.11, it is necessary to repeat selection of parameters until total length will be within the limits of the broken lines shown in Fig.11.

Drawing rules are schematically illustrated in Fig.16. No preferred orientation of fracture direction in the natural fracture patterns was observed. Therefore, the growth direction of fractures can be ignored except for the contact angle between branch fracture and the original fracture.  $\theta_1$  and  $\theta_m$  in Fig. 16 can be selected in the range from 0° to 180° using a random number generator, where  $\theta_m$  is the angle of straight line between junctions and  $\theta_1$  is representing the tortuosity of each fracture segment.  $\theta_1$  which is growth angle of branch fracture segment is also selected randomly, but  $\theta_1$  depends on  $\theta_m$  so that the bifurcated fractures grow on the both sides of the virtual extension of the preceding fracture.

Fig.17 shows examples of computer-generated fracture network model in the case of input fractal dimension 1.15. Output fractal dimensions are 1.20 and 1.13 respectively, similar to the input fractal dimension. The

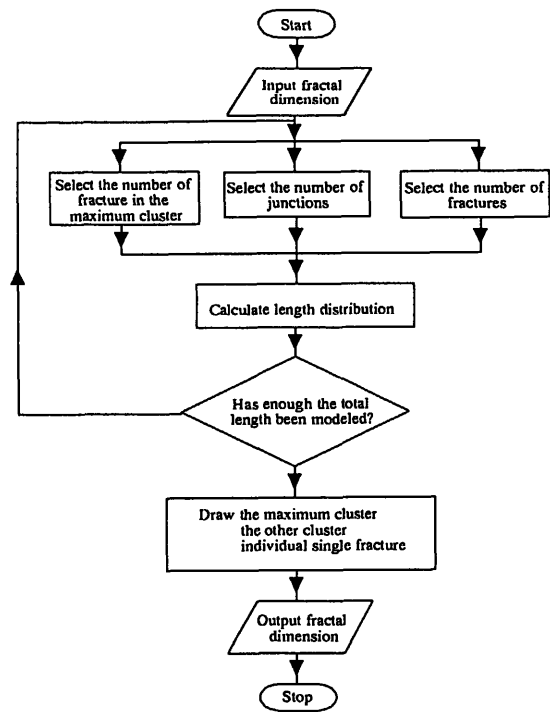


Fig.15 Flow chart for generation of fracture network model.

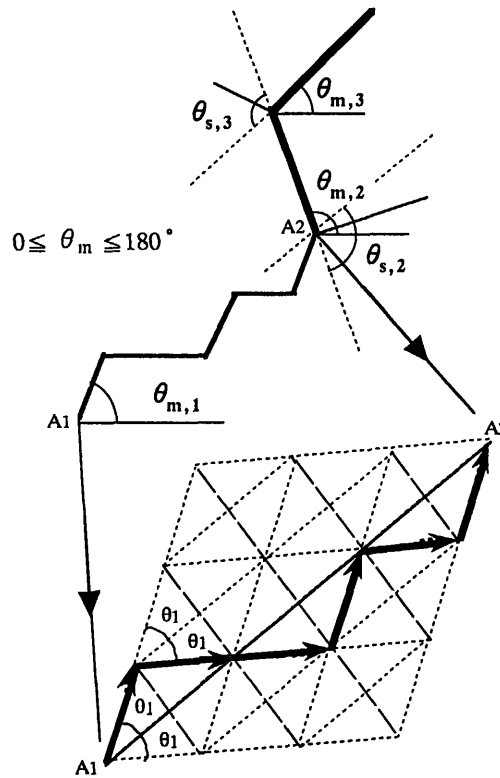


Fig.16 Schematic illustration fracture drawing.

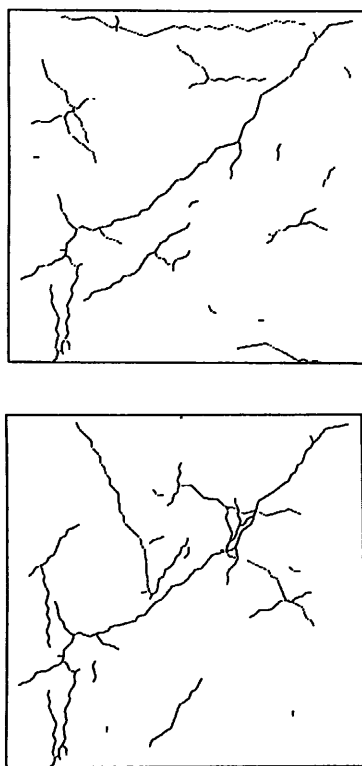


Fig.17 Examples of computer-generated fracture network model.

geometric features of these output patterns resemble those of the parent natural fracture patterns.

#### SUMMARY

The fracture distribution in the studied section of the Tamagawa Welded Tuffs shows fractal properties. Fractal dimensions of fracture space filling of 0.5m square observation areas fell within the limits 1.08 to 1.48. Length distribution, orientation, connectivity, the number of fractures and the total fracture length were measured to obtain the mutual relations between fractal dimension and the geometric features.

Using correlations between fractal dimension, the number of fractures in cluster<sub>max</sub>, number of junctions and number of fractures in whole fracture pattern, a two-dimensional fracture network model of given fractal dimension was generated without the consideration of fracture mechanics or the physical properties of the rocks. This computer-generated network was almost similar to the natural fracture patterns in rock sections with respect to fractal dimension, geometry and visual impression.

Tsuchiya et al.(1994) reported uniform fractal properties of fracture, space filling and shape, from microscopic to 10 meter scales in the same rocks. Therefore, it is possible that this artificial model could be expanded to the larger scales on the basis of self-similarity. We believe that such a modeling can be applied to simulate fractal fracture networks in natural geothermal reservoirs.

#### REFERENCES

Brown,S. R. and Scholz,C. H.,1985(a), Closure of random elastic surfaces in contact. *J.Geophys. Res.*, **90**, B7, 5531-5545.

Brown,S. R. and Scholz,C. H.,1985(b), Broad bandwidth study of the topography of natural rock surfaces. *J.Geophys. Res.*, **90**, B14, 12575-12582.

Chang,J. and Yortsos,Y.C.,1990, Pressure-Transient Analysis of Fractal Reservoirs: *SPE Formation Evaluation*, March, 31-38.

Katz,A.J. and Thompson,A.H., 1985, Fractal sandstone pores: Implications for conductivity and pore formation:*Physical Review Letters*,**54**, No.12, 1325-1328.

Klinkenberg,B., 1994, A review of methods used to determine the fractal dimension of linear features: *Mathematical Geology*, **26**, 23-46.

Ledésert,B. Dubois,J. Velde,B. Meunier,A. Genter A. and Badri,A., 1993, Geometrical and fractal analysis of a three-dimensional hydrothermal vein network in a fractured granite *J. Volcanology & Geothermal Res.*, **56**, 267-280.

Main,I.G., Peacock,S. and Meredith,P.G.,1990, Scattering attenuation and the fractal geometry of fracture systems: *PAGEOPH*, **133**, 283-304.

Matsukawa,Y., Tsuchiya,N and Nakatsuka K.,1995, Two-dimensional fracture network model in natural rock based on fractal analysis: *J.Geothermal Res. Soc.Japan*. (in Japanese with English abstract), submitted.

Odling,N.E.,1992, Network properties of a two-dimensional natural fracture pattern. *PAGEOPH*, **138**, 95-114.

Tamanyu,S. and Lanphere,M.A., 1983, Volcanic and geothermal history at the Hachimantai geothermal field in Japan -on the basis of K-Ar ages-: *J.Geol.Soc.Japan*, **89**, 501-510.

Tsang,Y.W. and Witherspoon,P.A., 1983, The Dependence of fracture mechanical and fluid flow properties on fracture roughness and sample size: *J.Geophys.Res.*, **88**, No.B3, 2359-2366.

Tsuchiya N., Matsukawa Y. and Nakatsuka K.,1994, Fractal analysis for space filling and shape of fractures in rock sections: *J.Geothermal Res.Soc. Japan*. **16**, 153-171.(in Japanese with English abstract)

Vaughan,Peter J.,Moore,Diane E.,Morrow,Carolyn A. and Byerlee, James D., 1986, Role of cracks in progressive permeability reduction during flow of heated aqueous fluids through granite: *J.Geophys.Res.*, **91**, No.B7, 7517-7530.

Watanabe K., and Takahashi H.,1995, Fractal geometry characterization of geothermal reservoir fracture networks: *J.Geophys.Res.* **100**, No.B, 521-528.